

Constraining 3-3-1 Models at the LHC and Future Hadron Colliders

A. Alves^{1,*}, L. Duarte^{7,†}, S. Kovalenko^{2,3,4,5,‡}, Y. M. Oviedo-Torres^{6,7,§}, F. S. Queiroz^{3,7,8,¶} and Y. S. Villamizar^{7,8,**}

¹*Departamento de Física, Universidade Federal de São Paulo, UNIFESP, Diadema, São Paulo, Brazil*

²*Departamento de Ciencias Físicas, Universidad Andres Bello, Sazie 2212, Piso 7, Santiago, Chile*

³*Millennium Institute for Subatomic Physics at High-Energy Frontier (SAPHIR), Fernandez Concha 700, Santiago, Chile*

⁴*Centro Científico-Tecnológico de Valparaíso, Casilla 110-V, Valparaíso, Chile*

⁵*Bogoliubov Laboratory of Theoretical Physics, JINR, 141980 Dubna, Russia*

⁶*Departamento de Física, Universidade Federal da Paraíba,*

Caixa Postal 5008, 58051-970, Joao Pessoa, PB, Brazil

⁷*International Institute of Physics, Universidade Federal do Rio Grande do Norte,*

Campus Universitario, Lagoa Nova, Natal-RN 59078-970, Brazil and

⁸*Departamento de Física, Universidade Federal do Rio Grande do Norte, 59078-970, Natal, RN, Brasil*

In this work, we derive lower mass bounds on the Z' gauge boson based on the dilepton data from LHC with 13 TeV of center-of-mass energy, and forecast the sensitivity of the High-Luminosity-LHC with $L = 3000 fb^{-1}$, the High-Energy LHC with $\sqrt{s} = 27$ TeV, and also at the Future Circular Collider with $\sqrt{s} = 100$ TeV. We take into account the presence of exotic and invisible decays of the Z' gauge boson to find a more conservative and robust limit, different from previous studies. We investigate the impact of these new decay channels for several benchmark models in the scope of two different 3-3-1 models. We found that in the most constraining cases, LHC with $139 fb^{-1}$ can impose $m_{Z'} > 4$ TeV. Moreover, we forecast HL-LHC, HE-LHC, and FCC-hh collider reach, and derived the projected bounds $m_{Z'} > 5.8$ TeV, $m_{Z'} > 9.9$ TeV, and $m_{Z'} > 27$ TeV, respectively. Lastly, we put our findings into perspective with dark matter searches to show the region of parameter space where a dark matter candidate with the right relic density is possible.

I. INTRODUCTION

Neutral resonances decaying to lepton pairs occur in several beyond the Standard Model (SM) theories that are motivated to explain open problems such as dark matter (DM), neutrino masses, parity violation and grand-unification, for example. Many of such models predict neutral gauge bosons, which can be produced at current and future colliders. In some dark matter models [1], Z' gauge bosons mediate interactions with the SM spectrum and are key to the dark matter phenomenology, as they can drive both the relic density and direct detection signals. A dark matter particle at the LHC is inferred from missing energy events, but the LHC can also indirectly contribute to the dark matter hunting by observing decays of those gauge bosons that mediate the DM-SM interactions. The dilepton channel is particularly interesting since it is much cleaner than the di-jet one, offering a better signal-over-background ratio.

From a collider physics perspective, obtaining mass bounds on a new vector boson is a promising strategy to assess which new physics models could be observed at the LHC. For instance, if a dilepton signal is observed with invariant mass at 4 TeV, one could conclude from our findings that such signal would not come from a model based on the $SU(3)_C \otimes SU(3)_L \otimes U(1)_X$ gauge symmetry, 3-3-1 for short.

Models based on this symmetry are phenomenologically compelling because may solve some open problems such as neutrino masses [2–16], dark matter [17–42], meson anomalies [43–50], flavor violation [51, 52], among others [53–58].

An important feature of these models is that the mass of the Z' gauge boson is determined by the energy scale at which the 3-3-1 symmetry breaks down to the 3-2-1. Furthermore, masses of the particles belonging to the 3-3-1 spectrum are also proportional to this energy scale. In other words, a bound on the Z' mass is seen as a limit on the entire 3-3-1 spectrum. For concreteness, we will focus our analysis on two popular models based on the 3-3-1 symmetry, namely 3-3-1 RHN and 3-3-1 LHN. As the symmetry suggests, the fermion content is arranged in triplets under $SU(3)_L$. In the 3-3-1RHN, the lepton triplet contains a right-handed neutrino, whereas the 3-3-1 LHN has a heavy neutral fermion. The key difference between these models is the presence of a viable dark matter candidate. In the latter, such heavy neutral fermion can reproduce the correct dark matter relic density and yield signals at direct detection experiments via interactions mediated by the Z' field. Therefore, a limit on the Z' boson translates into a constraint on possible dark matter signals. Lastly, 3-3-1 models have W' bosons, whose mass is also set by the energy scale of symmetry breaking, i.e., by the Z' mass. These new gauge boson can induce lepton flavor violation signals [36, 59], which again can be indirectly constrained by lower mass bounds on the Z' mass. We point out that 3-3-1 models naturally induce FCNC (flavor changing neutral currents) processes because one of the fermion generations transform differently under $SU(3)_L$. The FCNC processes stems from the Z' and scalar fields. It has been shown that scalars yield relatively smaller FCNC interactions [44, 47, 60]. That said, the B_d meson system in particular, can lead to strong constraints on the Z' mass depending on the parametrization used for the

* aalves@unifesp.br

† l.duarte@unesp.br

‡ sergey.kovalenko@unab.cl

§ ymot@estudantes.ufpb.br

¶ farinaldo.queiroz@ufrn.br

** yoxara@ufrn.edu.br

mixing matrices. Nevertheless, colliders offer an orthogonal and cleaner probe. Anyway, the discussion of FCNC in the context of 3-3-1 models is out of our scope. Therefore, limit ourselves to collider physics.

Dedicated collider studies of Z' bosons in the context of 3-3-1 models have been carried out in the past. A projected limit of 600 GeV has been derived in a linear collider [61]. In [62] the authors have derived the expected number of signal events for the LHC with $\sqrt{s} = 7, 14$ TeV. A similar study was done in [63], but focusing on a doubly charged vector boson present in some 3-3-1 models whose mass is connected to the Z' . Hence, one could treat it as an indirect probe for Z' bosons. In [64] the authors derived an indirect lower mass bound on the Z' gauge boson using the mass relation between the Z' and the vector doubly charged gauge boson in a 3-3-1 model. In [65] two lower Z' mass bounds, 2.2 TeV and 2.5 TeV, were obtained from the LHC data using different 3-3-1 models. In [66] a more updated analysis has been carried out but again focused on the doubly charged gauge boson. In [47] and [59] the authors derived a lower mass limit, 3 – 4 TeV, on the Z' boson considering only Z' decays into charged leptons. A discussion concerning the relevance of exotic Z' decays has been already raised in [67], but a solid calculation was still missing. Hence, it is clear that an updated and comprehensive derivation of lower mass limits on the Z' gauge boson belonging to 3-3-1 models was missing up to now.

Motivated by the importance of the Z' gauge boson to 3-3-1 constructions, we compute lower mass bounds on Z' boson based on dilepton decays, $Z' \rightarrow \ell^+ \ell^-$, $\ell = e, \mu$, for both 3-3-1RHN and 3-3-1LHN models using 139 fb^{-1} of data collected from proton-proton collisions at the 13 TeV [68] taking into account overlooked exotic decays, such as decay into exotic quarks and dark matter. These new decay channels might significantly impact the lower bound obtained considering only decays into SM fermions as previously assumed [47, 59, 61–66]. We assess the relevance of these new decay channels for several benchmark models. Furthermore, under the assumption that no positive signal is found, we forecast limits for the High-Luminosity (HL) and High-Energy (HE) LHC setups, HL-LHC and HE-LHC, respectively, as well as for the Future Circular Collider (FCC-hh). Lastly, in the context of the 3-3-1 LHN model, we investigate if one can host a viable dark matter candidate in light of those bounds.

In summary, our present work expands previous studies in the following directions:

1. taking into account updated data from LHC,
2. considering HL-LHC, HE-LHC and FCC setups
3. contemplating overlooked Z' decays,
4. connecting our findings with dark matter phenomenology.

This work is organized as follows: in *Section II* we review the 3-3-1 model and the relevant Z' decay channels; in *Section III* we discuss the benchmark models and kinematic

cuts used in the production of the Z' signal; in *Section IV* we present our collider findings; in *Section V* we connect our collider results with dark matter phenomenology; and finally in *Section VI* we draw our conclusions.

II. 3-3-1 RHN AND LHN MODELS

A. Fermion Content

In our work we analyze two models based on the local symmetry group $\mathbf{SU(3)}_C \times \mathbf{SU(3)}_L \times \mathbf{U(1)}_X$, namely 3-3-1 with right-handed neutrinos (3-3-1 RHN), [69, 70], and 3-3-1 with neutral left-handed fermion (3-3-1 LHN) [20, 71]. The electric charge operator in these two models is the same,

$$\frac{Q}{e} = \frac{1}{2} \left(\lambda_3 - \frac{1}{\sqrt{3}} \lambda_8 \right) + X \cdot \hat{1}, \quad (1)$$

where $\lambda_{3,8}$, are the diagonal generators of $\mathbf{SU(3)}_L$ and $\hat{1}$ is the identity matrix that acts as a generator of $\mathbf{U(1)}_X$ group with X being its corresponding charge.

The **3-3-1 RHN** model contains triplet and singlet fermionic fields with the following $\mathbf{SU(3)}_C \times \mathbf{SU(3)}_L \times \mathbf{U(1)}_X$ assignments:

$$f_{aL} = \begin{pmatrix} \nu_L^a \\ \ell_L^a \\ \nu_R^{ac} \end{pmatrix} \sim (1, 3, -1/3), \quad \ell_{aR} \sim (1, 1, -1), \quad (2)$$

$$Q_{iL} = \begin{pmatrix} d_i \\ -u_i \\ d_i' \end{pmatrix}_L \sim (3, \bar{3}, 0), \quad u_{iR} \sim (3, 1, 2/3), \quad (3)$$

$$d_{iR} \sim (3, 1, -1/3), \quad d_i' \sim (3, 1, -1/3),$$

$$Q_{3L} = \begin{pmatrix} u_3 \\ d_3 \\ T \end{pmatrix}_L \sim (3, 3, 1/3), \quad u_{3R} \sim (3, 1, 2/3), \quad (4)$$

$$d_{3R} \sim (3, 1, -1/3), \quad T_R \sim (3, 1, 2/3),$$

where $a = 1, 2, 3$ and $i = 1, 2$ indicate the generation indices. Notice that we have three new exotic quarks q' (d_i' and T).

In the **3-3-1 LHN** a new heavy neutral lepton N_L^a replaces the $(\nu_R^a)^c$ in the lepton triplet. Besides, a right-handed neutral fermion N_R^a is introduced, transforming as a singlet under $\mathbf{SU(3)}_L$,

$$N_R^a \sim (1, 1, 0), \quad (5)$$

but the quark sector remains unchanged.

Z' Interactions in the 3-3-1 model		
Interaction	g'_V	g'_A
$Z' \bar{u}u, \bar{c}c$	$\frac{3 - 8 \sin^2 \theta_W}{6\sqrt{3 - 4 \sin^2 \theta_W}}$	$-\frac{1}{2\sqrt{3 - 4 \sin^2 \theta_W}}$
$Z' \bar{t}t$	$\frac{3 + 2 \sin^2 \theta_W}{6\sqrt{3 - 4 \sin^2 \theta_W}}$	$-\frac{1 - 2 \sin^2 \theta_W}{2\sqrt{3 - 4 \sin^2 \theta_W}}$
$Z' \bar{d}d, \bar{s}s$	$\frac{3 - 2 \sin^2 \theta_W}{6\sqrt{3 - 4 \sin^2 \theta_W}}$	$-\frac{3 - 6 \sin^2 \theta_W}{6\sqrt{3 - 4 \sin^2 \theta_W}}$
$Z' \bar{b}b$	$\frac{3 - 4 \sin^2 \theta_W}{6\sqrt{3 - 4 \sin^2 \theta_W}}$	$-\frac{1}{2\sqrt{3 - 4 \sin^2 \theta_W}}$
$Z' \bar{\ell}\ell$	$\frac{-1 + 4 \sin^2 \theta_W}{2\sqrt{3 - 4 \sin^2 \theta_W}}$	$\frac{1}{2\sqrt{3 - 4 \sin^2 \theta_W}}$
$Z' \bar{N}N$	$\frac{4\sqrt{3 - 4 \sin^2 \theta_W}}{9}$	$-\frac{4\sqrt{3 - 4 \sin^2 \theta_W}}{9}$
$Z' \bar{\nu}_\ell \nu_\ell$	$\frac{\sqrt{3 - 4 \sin^2 \theta_W}}{18}$	$-\frac{\sqrt{3 - 4 \sin^2 \theta_W}}{18}$
$Z' \bar{d}_i^i d_i^i$	$-\frac{3 - 5 \sin^2 \theta_W}{3\sqrt{3 - 4 \sin^2 \theta_W}}$	$\frac{1 - \sin^2 \theta_W}{\sqrt{3 - 4 \sin^2 \theta_W}}$
$Z' \bar{T}T$	$\frac{3 - 7 \sin^2 \theta_W}{3\sqrt{3 - 4 \sin^2 \theta_W}}$	$-\frac{1 - \sin^2 \theta_W}{\sqrt{3 - 4 \sin^2 \theta_W}}$

Table I. Vector and Axial couplings of the Z' boson with fermions in the 3-3-1 RHN and LHN models. In the 3-3-1 RHN model there are no interactions with the heavy fermions N. Apart from that, the Z' interactions are precisely the same as the 3-3-1 LHN model.

B. Scalar Sector

Fermion masses are obtained through the introduction of three scalar triplets, which we denote as χ , ρ and η [20],

$$\begin{aligned}
\chi &= \begin{pmatrix} \chi^0 \\ \chi^- \\ \chi'^0 \end{pmatrix} \sim (1, 3, -1/3), & \langle \chi \rangle &= \begin{pmatrix} 0 \\ 0 \\ v_\chi \end{pmatrix}, \\
\rho &= \begin{pmatrix} \rho^+ \\ \rho^0 \\ \rho'^+ \end{pmatrix} \sim (1, 3, 2/3), & \langle \rho \rangle &= \begin{pmatrix} 0 \\ v_\rho \\ 0 \end{pmatrix}, \\
\eta &= \begin{pmatrix} \eta^0 \\ \eta^- \\ \eta'^0 \end{pmatrix} \sim (1, 3, -1/3), & \langle \eta \rangle &= \begin{pmatrix} v_\eta \\ 0 \\ 0 \end{pmatrix}.
\end{aligned} \tag{6}$$

where v_χ , v_ρ and v_η correspond to the vacuum expectation values (VEVs) defining a two-step spontaneous symmetry breaking (SSB)

$$\text{SU}(3)_L \times \text{U}(1)_X \xrightarrow{\langle \chi \rangle} \text{SU}(2)_L \times \text{U}(1)_Y \xrightarrow{\langle \eta \rangle, \langle \rho \rangle} \text{U}(1)_Q.$$

They form the scalar potential,

$$\begin{aligned}
V(\eta, \rho, \chi) &= \mu_\chi^2 \chi^2 + \mu_\eta^2 \eta^2 + \mu_\rho^2 \rho^2 + \lambda_1 \chi^4 + \lambda_2 \eta^4 + \lambda_3 \rho^4 + \\
&\lambda_4 (\chi^\dagger \chi) (\eta^\dagger \eta) + \lambda_5 (\chi^\dagger \chi) (\rho^\dagger \rho) + \lambda_6 (\eta^\dagger \eta) (\rho^\dagger \rho) + \\
&\lambda_7 (\chi^\dagger \eta) (\eta^\dagger \chi) + \lambda_8 (\chi^\dagger \rho) (\rho^\dagger \chi) + \lambda_9 (\eta^\dagger \rho) (\rho^\dagger \eta) \\
&- \frac{f}{\sqrt{2}} \epsilon^{ijk} \eta_i \rho_j \chi_k + \text{H.c.}
\end{aligned} \tag{7}$$

We have assumed $f = v_\chi$, $\lambda_2 = \lambda_3$, $\lambda_4 = \lambda_5$ to simplify our analytical results, but our conclusions are based on pre-

cise numerical calculations, where these simplifying assumptions are not made. The CP-even scalars give rise to the mass eigenstates, S_1 , S_2 and the Higgs boson, with the following masses,

$$\begin{aligned}
m_{S_1}^2 &= \frac{v^2}{4} + 2\lambda_1 v_\chi^2, \\
m_{S_2}^2 &= (v_\chi^2 + 2v^2(2\lambda_2 - \lambda_6)) / 2, \\
m_H^2 &= v^2(2\lambda_2 + \lambda_6),
\end{aligned} \tag{8}$$

whereas only a pseudoscalar mass eigenstate survives, P_1 , where

$$m_{P_1}^2 = \frac{1}{2}(v_{\chi'}^2 + \frac{v^2}{2}). \tag{9}$$

A complex neutral scalar ϕ which is a combination of χ^0 and η'^0 arises, as well as two charged scalars h_1 and h_2 whose masses are found to be,

$$m_\phi^2 = \frac{(\lambda_7 + \frac{1}{2})}{2} [v^2 + v_{\chi'}^2], \tag{10}$$

$$\begin{aligned}
m_{h_1^-}^2 &= \frac{\lambda_8 + \frac{1}{2}}{2} (v^2 + v_{\chi'}^2), \\
m_{h_2^-}^2 &= \frac{v_{\chi'}^2}{2} + \lambda_9 v^2.
\end{aligned} \tag{11}$$

These scalars are not relevant to our reasoning, but to clearly show this we will need Eqs.(8)-(11) and the gauge boson masses that we will cover below.

Table II. Implemented benchmark sets (BMs) corresponding to mass values of the heavy exotic quarks q' and the heavy neutral lepton N in the 3-3-1 RHN and LHN models.

Model	3-3-1 LHN	3-3-1 RHN
Mass	$M_{q'}$ [TeV]	M_N [TeV]
BM1	10	10
BM2	1	10
BM3	1.5	10
BM4	2	10
BM5	2	2
BM6	2	2.5
BM7	2	4
BM8	1	1
BM9	0.5	10
BM10	10	0.5

C. Gauge Bosons

Throughout, we adopt the decoupling limit where the energy scale of SSB of the 3-3-1 symmetry is much larger than

the electroweak one, i.e., $v_\chi \gg v_\eta, v_\rho$. As a result of the enlarged gauge group, new gauge bosons arise: W'^{\pm}, U^0 , and a Z' . Their masses are given by,

$$m_{Z'}^2 = \frac{g^2}{(3 - 4s_W^2)} \left(c_W^2 v_\chi^2 + \frac{v_\rho^2 + v_\eta^2 (1 - 2s_W^2)^2}{4c_W^2} \right),$$

$$m_{W'}^2 = \frac{g^2}{4} (v_\eta^2 + v_\chi^2), \quad m_{U^0}^2 = \frac{g^2}{4} (v_\rho^2 + v_\chi^2), \quad (12)$$

where $v^2 = v_\eta^2 + v_\rho^2 \simeq 246$ GeV, g is the $SU(2)_L$ gauge coupling, $c_W \equiv \cos\theta_W$, $s_W \equiv \sin\theta_W$, with θ_W being the Weinberg angle. From Eq. (12), one can clearly see that the gauge boson masses are determined by v_χ . Hence, once we set a bound on the Z' mass, it can be translated into a constraint on the W' and U^0 masses as well. One should notice that W' , Z' and U^0 bosons have similar masses.

We derive the limit on the Z' mass using the high-mass dilepton resonance searches at the ATLAS detector with $\sqrt{s} = 13$ TeV center-of-mass-energy, and later estimate the future collider bounds. In that regard, the main ingredient is the neutral current that reads

$$\mathcal{L}_{Z'ff}^{NC} = \frac{g}{2c_W} \bar{f} \gamma^\mu \left[g_V^{(f)} + \gamma_5 g_A^{(f)} \right] f Z'_\mu, \quad (13)$$

where $g_V^{(f)}$ and $g_A^{(f)}$ are the vector (axial) coupling constant of fermions $f = \ell, N, q'$ with Z' (see Table I). The branching ratio of the Z' boson in two charged leptons is defined as

$$\text{Br}(Z' \rightarrow \ell\bar{\ell}) = \frac{\Gamma(Z' \rightarrow \ell\bar{\ell})}{\Gamma_{Z'}}, \quad (14)$$

where $\Gamma_{Z'}$ is the total width

$$\Gamma_{Z'} = \sum_X \Gamma(Z' \rightarrow 2X), \quad (15)$$

being X the SM particles and new particles in 3-3-1 models. The $\Gamma(Z' \rightarrow \ell\bar{\ell})$ is the partial decay width into dileptons at leading order, with $\ell = e, \mu$,

D. Importance of Scalars and Gauge Boson Decays

The decay widths were actually computed using CalcHEP [72]. As we pointed out before, our calculation of the total width takes into account all possible decays, including new gauge bosons, scalars, exotic quarks and dark matter whenever they are allowed.

We have written explicitly the scalar masses to address the relevance of scalar fields to our reasoning. Bear in mind $m_{Z'} \simeq 0.3v_\chi$, and the relevant Z' interactions are: $Z'\phi\phi^*$, $Z'W'h_1^-, Z'h_1^-h_1^+, Z'h_2^-h_2^+, Z'W^+h_2^-, Z'P_1S_1$, among others. Looking at Eq.8-11 it is clear that the scalars are much more massive than the Z' gauge boson, and thus do not contribute to the two-body Z' decay width. Three-body decays widths are possible, but suppressed. For this reason, we

can solidly state that scalars do not play a role in our phenomenology. Moreover, as the exotic gauge bosons have similar masses, Z' decays into exotic boson pairs are not kinematically accessible. There are exotic decays into dark matter and exotic quarks that are important, however, but we will address in the next section. Furthermore, as the scalar are much more massive than the Z' gauge boson, they are not within reach LHC. In summary, scalar fields do not offer a possible signature for a 3-3-1 symmetry at the LHC.

III. DATA AND SIGNAL OUTPUT

We carry out our collider simulation with Madgraph5 [73, 74], and compute the decay with CalcHEP [72, 75]. We compute the $pp \rightarrow Z' \rightarrow \ell\bar{\ell}$ at $\sqrt{s} = 13$ TeV, with $\ell = e, \mu$ and compare our findings with the public results from ATLAS Collaboration [68]. We generate the Monte Carlo events to simulate the cross-section of the Drell-Yan process using the parton distribution function (PDF) NNPDF23LO [76]. We require two opposite charge leptons in the event and the following kinematic cuts in order to compare our results with the ATLAS Collaboration data: $p_T > 30$ GeV¹ and $|\eta| < 2.5$ ².

Instead of considering only Z' interactions to fermions as done in previous works, we fully implemented the model in LANHEP [77–79], SARAH-HEP [80–82] and Feynrules [83, 84] to generate the output files for CalcHEP and Madgraph5, respectively. This is important because additional exotic decays of the Z' gauge boson can significantly weaken the lower mass bounds based on dilepton data. The more sizeable decay channels are added to the total width, the smaller is the branching ratio into dileptons. Consequently, weaker limits are found. We investigate the importance of each of the possible new decay channels by considering several benchmark models.

A. Importance of exotic Z' decays and benchmarks models

In the 3-3-1 models explored here, the Z' might decay into SM fermions, new scalars, new gauge bosons ($W'^{\pm}, U^0, U^{0\prime}$), and invisibly (N_i). One of the three heavy fermions is cosmologically stable, and is rendered as dark matter candidate. The other two are long-lived. Suppose N_1 is the lightest one, for the sake of the argument. Because of a Z_2 symmetry where $N_i \rightarrow -N_i$, N_2 might decay into N_1 via the W' gauge boson, but this decay width is suppressed for two reasons: the W' is heavy, and second, the entries of the mixing matrix involving $N_1 - N_2 - N_3$ should also be small otherwise one could observe lepton flavor violation processes as explored in

¹ Transverse momentum is the component of the momentum that is perpendicular to the beam axis.

² The pseudo-rapidity η is defined as, $\eta = -\ln \tan \frac{\theta}{2}$, where θ is the polar angle between the particle's linear momentum and the positive direction of the beam axis.

[36]. As far as collider searches are concerned, without worrying about particular details of the masses and mixing matrices, we can safely take the neutral fermions as stable particle, and thus rendered as missing energy.

We have checked that decays into new scalars and exotic gauge bosons are either very suppressed or kinematically prohibited for the benchmark points of Table II. Hence, the only relevant new decay channels beyond the SM, are those involving exotic quarks, and neutral fermions (N_i).

Hence, we investigate several benchmark models varying the masses of the decay products to quantify their importance in the derivation of lower mass bounds.

B. Methods

We compute the $\sigma \times \text{BR}(\ell\bar{\ell})$ at the LHC using the aforementioned high-energy physics tools for each benchmark model (BM) in Table II, and later compare our results with ATLAS data. Furthermore, we use these results to obtain, new bounds for HL-LHC, HE-LHC and FCC-hh colliders. To this end we apply Collider Reach (β) tool, which takes the input bound on $m_{Z'}$ obtained in the first step at a certain center-of-mass-energy and luminosity, and forecasts new bounds for a different collider configurations including center-of-mass-energy and luminosity. In our work, we are interested in the High-Luminosity, High-Energy [85], and the FCC proton-proton setups [86].

IV. RESULTS AND DISCUSSIONS

a. Branching ratios. The partial widths of the Z' into charged leptons is the same for both 3-3-1 models, as they have identical interactions (see Eq. (13), and Table I), yet the branching ratio into charged leptons can be quite different for these two models. The key difference of the 3-3-1 LHN from the 3-3-1 RHN is the presence of heavy neutral fermions, N_i . Only when decays into N_i pairs are inaccessible, both models are indistinguishable as far as $Z' \rightarrow \ell^+\ell^-$ searches are concerned. As aforementioned, section III A, the scalars are not relevant to our results. Despite decays to scalars are present in some benchmarks, they are negligible compared to decays into SM quarks and leptons.

We have shown in Figs. 1, 2, 3, and 4 the branching ratio $\text{BR}(Z' \rightarrow \ell\bar{\ell})$ as a function of $m_{Z'}$ for several BM in the 3-3-1 RHN and LHN models. We notice that in both models, the value of the branching ratio is less than 2% and 1.7%, respectively. In Fig. 1, for the 3-3-1 LHN, the BM 2-3-4 lead to a drop near 2000 GeV, 3000 GeV, and 4000 GeV, respectively. This behavior is caused by Z' decay into exotic quark. In contrast, the BM1 does not experience such behavior since the new exotic quarks masses are fixed at 10 TeV.

In the same way, for the 3-3-1 LHN model, we observed some substantial decrease in the branching ratio into charged leptons for the BM sets 5, 6, and 7 when $m_{Z'} = 4000$ GeV (see Fig. 2). It has to do with the exotic quarks at $m_{q'} = 2000$ GeV. The importance of decays into heavy neutral

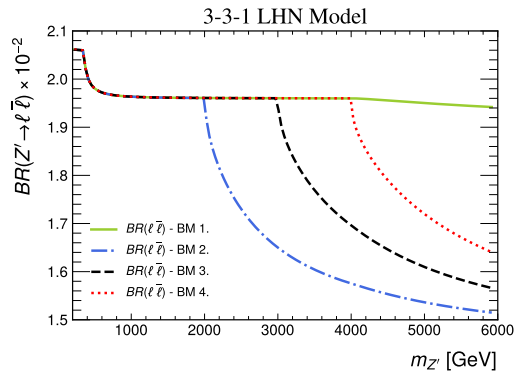


Figure 1. Branching ratio for the Z' decay into dilepton channel as a function to $m_{Z'}$ for the benchmark sets BM1, BM2, BM3, and BM4 of the 3-3-1 LHN model.

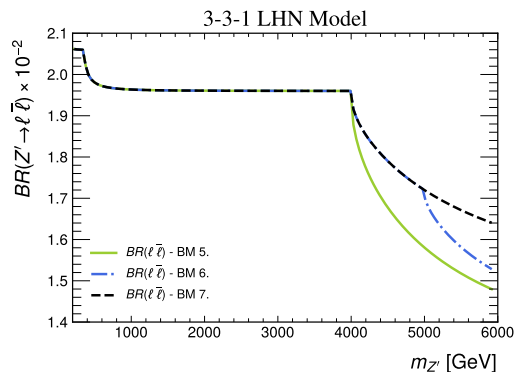


Figure 2. Branching ratio for the Z' decay into dilepton channel as a function of $m_{Z'}$ for the benchmark sets BM 5, 6 and 7 of the 3-3-1 LHN model.

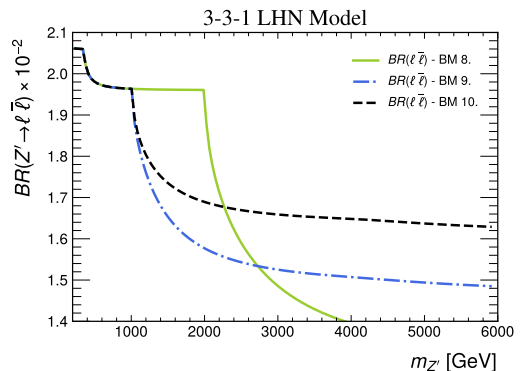


Figure 3. Branching ratio for the Z' decay into dilepton channel as a function to $m_{Z'}$ for the benchmark sets BM 8, 9, and 10 the 3-3-1 LHN model.

fermions can be seen in BM 6, which leads to a significant decrease in the branching ratio when $m_{Z'} \sim 5$ TeV, as we fixed $m_{N_i} = 2.5$ TeV. In a similar vein, the behavior seen in Fig. 3 can be explained.

For the 3-3-1 RHN model, we observe that the behavior for

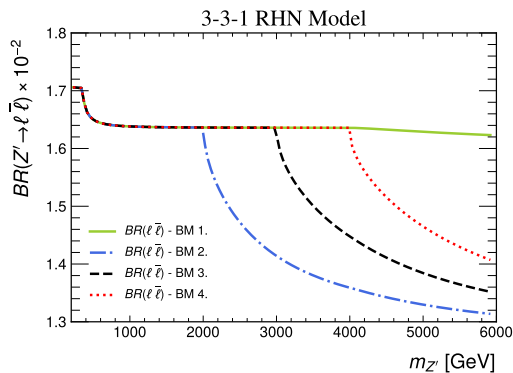


Figure 4. Branching ratio for the Z' decay into dilepton channel as a function to $m_{Z'}$ for the 3-3-1 RHN model.

Table III. $m_{Z'}$ lower bounds taking into account the dilepton signal data at the LHC [68] and the theoretical signal production from Fig. 5 for the 3-3-1 RHN and LHN models.

Model	BM	$m_{Z'}$ [GeV]
3-3-1 RHN	BM 1 ^a	4052
	BM 2	3960
	BM 3 ^b	3989
	BM 4	4040
3-3-1 LHN	BM 1	4132
	BM 2	4013
	BM 3	4060
	BM 4, 6 and 7	4118
	BM 5	4094
	BM 8	3950

^a The lower bounds of BM 1 for the 3-3-1 RHN model are equivalent to those of BM 10 in the 3-3-1 LHN model.

^b The lower bound of BM 3 for the 3-3-1 RHN model is equivalent to those of BM 9 in the 3-3-1 LHN model.

the branching ratio is similar to the 3-3-1 LHN model since by performing the same variations on the exotic quark masses, we have the same decrease in the branching ratio (see Fig. 4). However, the size of the branching ratio into charged leptons is smaller because the Z' can always decay into right-handed neutrinos, which are assumed to have keV masses [87].

b. Signal production As explained above, the theoretical production of an Z' at the LHC decaying into dileptons was generated using MadGraph5 and CalcHEP. To compare the theoretical signal for the dilepton channel Z' with ATLAS collaboration data presented in Fig. 3(a) in [68], we plot $\sigma(pp \rightarrow Z') \times BR(Z' \rightarrow \ell\bar{\ell})$ as a function of $m_{Z'}$ for the 3-3-1 RHN and LHN models, as seen in Fig. 5. For the Z' mass we take different values in the interval of $200 \text{ GeV} < m_{Z'} < 6000 \text{ GeV}$ with steps of 40 GeV. The lower mass bounds on the Z' are obtained by considering the intersection of the solid yellow-green, dash-dot blue, and black dotted lines with the red solid curve in Figs. 5(a), 5(b), 5(c) and 5(d), and these results are summarized in Table III.

c. HE-HL and FCC-hh colliders. After obtaining the lower bounds of $m_{Z'}$ for the 13 TeV LHC after 139 fb^{-1} (Table III), we use these results as input for Collider Reach

(β) with the PDF MMHTMMHT2014nnlo68c1 [88], and obtain the expected limits for HL-LHC, HE-LHC and FCC-hh setups.

We set the following collider configurations:

- HE-HL : for the center-of-mass energy $\sqrt{s} = 13 \text{ TeV}$, 14 TeV and 27 TeV, and integral luminosity $L_{int} = 139 \text{ fb}^{-1}$, 300 fb^{-1} , 500 fb^{-1} , and 3000 fb^{-1} .
- FCC-hh: for the center-of-mass energy $\sqrt{s} = 100 \text{ TeV}$ and integral luminosity $L_{int} = 139 \text{ fb}^{-1}$, 300 fb^{-1} , 500 fb^{-1} , and 3000 fb^{-1} .

The mass reach, are displayed in Table IV for HE-HL and FCC-hh collider. At the HL-LHC, the expected lower mass bounds raise by 1.2–1.5 TeV compared to the 139 fb^{-1} data. Table III. In special, with 3000 fb^{-1} at the 14 TeV LHC, the projected sensitivity increases by almost 2 TeV compared to the current bounds for some benchmark points.

At the 27 TeV HE-LHC and the 100 TeV FCC-hh collider, with $L_{int} = 3000 \text{ fb}^{-1}$, the lower mass bounds improve by a factor of ~ 2.5 and ~ 7 , respectively, compared to those obtained at the LHC with a center-of-mass energy $\sqrt{s} = 13 \text{ TeV}$ and integral luminosity of 139 fb^{-1} (see Table III).

We also note that BM 1 and 3, in the 3-3-1 RHN model, coincide with BM 10 and 9 in the 3-3-1 LHN model, respectively. Moreover, BM 6-7 present a similar bound to BM 4 in the 3-3-1 LHN model, and these results are easily justified by the presence or not of exotic Z' decays as discussed previously.

Having in mind that 3-3-1 LHN features heavy neutral fermions that can be dark matter candidates, one may wonder if the current and projected collider bounds derived in our work preclude the existence of a plausible dark matter candidate in the model. We address this concern below.

V. DARK MATTER

a. Thermal Production The lightest of the neutral fermions, let us say N_1 , can be a viable dark matter candidate due to a Z_2 symmetry [20, 22]. The dark matter abundance is governed by s-channel annihilations into SM fermions mediated by the Z' gauge field. The Z' interactions with SM fermions are set by the gauge symmetry, which features a fixed gauge coupling. In other words, the dark matter abundance is governed by two parameters only, the dark matter and the Z' masses [20, 42]. Furthermore, the dark matter scattering off nucleon occurs through a t-channel Z' exchange. Hence, the dark matter phenomenology is quite predictable once we fix the Z' mass.

In the context of thermal production, where the production of dark matter occurs in the usual standard freeze-out, the curve that yields the correct relic density, $\Omega h^2 = 0.11$ [89], is shown in Fig. 6 with solid blue curves. We also exhibit the region where the dark matter is overabundant and underabundant. Considering current LHC bound, we observe that for the BM 5, $m_N = 2 \text{ TeV}$, we can reproduce the correct relic density for $m_{Z'} \sim 4.6 \text{ TeV}$, which safely obeys LHC constraints. However, with 500 fb^{-1} of data, LHC will already

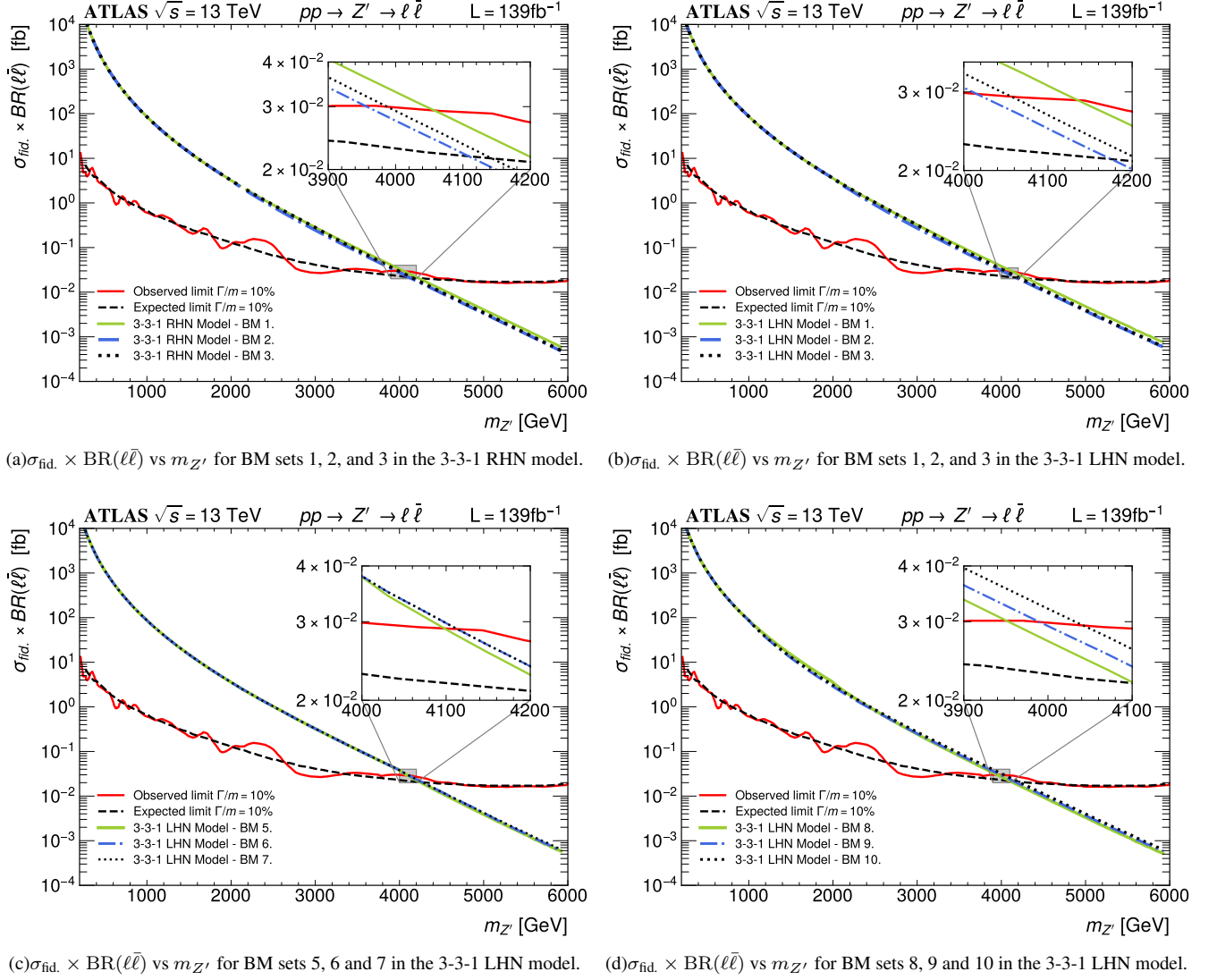


Figure 5. Solid red and dashed black lines symbolize $\sigma_{\text{fid.}} \times \text{BR}(\ell\bar{\ell})$ upper limits observed and expected at 95%CL as a function of Z' mass for the 10% width signals for the dilepton channel $Z' \rightarrow \ell\bar{\ell}$ in the ATLAS experiment at a center of mass energy 13 TeV (ATLAS Collaboration [68]). The solid yellowgreen, dash-dot blue, and black dotted lines represent the theoretical production $\sigma(pp \rightarrow Z') \times \text{BR}(Z' \rightarrow \ell\bar{\ell})$ generated using MadGraph5 and CalcHEP for several benchmark sets for the 3-3-1 RHN and LHN models. We assume different masses for the new exotic quarks and heavy neutral lepton (see Table II). The lower mass bounds on the Z' obtained can be seen in Table III.

be able to probe this scenario (see Table IV). For the BM 6, the right relic density is found for $m_{Z'} \sim 4.7$ and 5.7 TeV, whereas for BM7 a 5.8 TeV, 7.8 TeV and 8.8 TeV Z' could yield the correct relic density. In particular, for the BM 1, only HE-LHC has the potential to fully probe this scenario, as it can exclude Z' masses up to 9.8 TeV. There are many interesting scenarios to be explored, but one can solidly see the importance of orthogonal and complementary searches for new physics. Our study, clearly shows that setting aside one's theoretical prejudice for multi-TeV mediators, vanilla thermal dark matter models, such as the one present in the 3-3-1 LHN model, is fully consistent with current LHC data, and only the next generation of colliders will be able to close the few TeV dark matter particle window.

b. Direct Detection The neutral fermion can indeed leave signals at direct detection experiments through t-channel Z' exchange, but the limits are weak compared to those stemming from collider searches. This is a typical feature of vector mediator models that have sizeable couplings to fermions [90, 91]. The current and projected direct detection bounds, from XENON or PANDAX collaborations [92–94] are significantly surpassed by current LHC data, mainly when are put into perspective with future colliders. For this reason, we decided not to show them in Fig. 6.

Table IV. $m_{Z'}$ mass reach for all benchmark sets considered in this work at HE-HL and FCC-hh colliders by increasing the center-of-mass energy (\sqrt{s}) from 13TeV until 100TeV, and integral luminosity (L_{int}) from $139 fb^{-1}$ to $3000 fb^{-1}$, for the 3-3-1 RHN and LHN models. Values of $m_{Z'}$ for HE-HL LHC appear between the fourth and sixth columns of the table, whereas for the FCC-hh collider, the $m_{Z'}$ reaches are shown in the seventh column, when increasing the luminosity (column three).

Model	Benchmark (BM) sets	$L_{int}[fb^{-1}]$	$m_{Z'}[TeV]-13TeV$	$m_{Z'}[TeV]-14TeV$	$m_{Z'}[TeV]-27TeV$	$m_{Z'}[TeV]-100TeV$
3-3-1 RHN	BM 1 ^a	139	4.052	4.288	6.987	17.180
		300	4.390	4.651	7.675	19.447
		500	4.613	4.892	8.136	21.006
		1000	4.916	5.217	8.763	23.175
		3000	5.388	5.727	9.755	26.711
	BM 2	139	3.960	4.189	6.801	16.548
		300	4.298	4.552	7.487	18.821
		500	4.521	4.793	7.947	20.363
		1000	4.825	5.119	8.574	22.514
		3000	5.298	4.699	9.566	26.030
	BM 3 ^b	139	3.989	4.220	6.860	16.769
		300	4.327	4.583	7.547	19.016
		500	4.550	4.824	8.006	20.564
		1000	4.853	5.149	8.633	22.721
		3000	5.326	5.661	9.626	26.244
	BM 4	139	4.040	4.275	6.963	17.101
		300	4.378	4.638	7.651	19.364
		500	4.601	4.879	8.111	20.921
		1000	4.904	5.204	8.739	23.089
		3000	5.377	5.715	9.731	26.652
3-3-1 LHN	BM 1	139	4.132	4.374	7.149	17.709
		300	4.470	4.737	7.839	19.990
		500	4.693	4.978	8.301	21.571
		1000	4.995	5.303	8.928	23.755
		3000	5.467	5.812	9.920	27.306
	BM 2	139	4.013	4.246	6.908	16.924
		300	4.351	4.609	7.596	19.197
		500	4.574	4.850	8.056	20.731
		1000	4.877	5.175	8.683	22.894
		3000	5.350	5.686	9.675	26.421
	BM 3	139	4.060	4.297	7.003	17.233
		300	4.398	4.660	7.692	19.502
		500	4.621	4.901	8.153	21.062
		1000	4.924	5.225	8.780	23.233
		3000	5.396	5.736	9.772	26.770
	BM 4, 6, and 7	139	4.118	4.359	7.121	17.616
		300	4.456	4.722	7.811	19.902
		500	4.679	4.963	8.272	21.472
		1000	4.981	5.288	8.900	23.654
		3000	5.453	5.797	9.891	27.202
	BM 5	139	4.094	4.333	7.072	17.457
		300	4.432	4.696	7.761	19.736
		500	4.655	4.937	8.223	21.302
		1000	4.958	5.262	8.850	23.479
		3000	5.430	5.772	9.842	27.023
	BM 8	139	3.950	4.178	6.781	16.520
		300	4.288	4.541	7.467	18.753
		500	4.511	4.782	7.926	20.294
		1000	4.815	5.108	8.553	22.443
		3000	5.289	5.620	9.546	25.956

^a The lower bounds of BM 1 for the 3-3-1 RHN model are equivalent to those of BM 10 in the 3-3-1 LHN model.

^b The lower bounds of BM 3 for the 3-3-1 RHN model are equivalent to those of BM 9 in the 3-3-1 LHN model.

VI. CONCLUSIONS

In this work, we derived LHC bounds on two different 3-3-1 models, namely 3-3-1 RHN and 3-3-1 LHN. We assessed

the impact of overlooked exotic Z' decays in the derivation of lower mass limits using dilepton data. Later, we obtained solid lower mass bounds that range from 3.9 TeV to 4.1 TeV, signif-

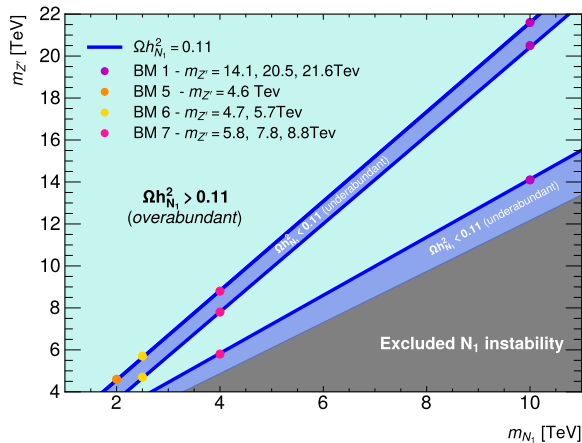


Figure 6. Parameter space $m_{Z'} \times m_{N_1}$ plane that explains the thermal relic density. BM models are indicated in the figure, as well the regions that lead to overabundant and underabundant dark matter. In the gray region, N_1 is not stable.

icantly weaker than previous studies. We also forecasted HL-LHC, HE-LHC and FCC-hh mass reach, and put our results into perspective with dark matter phenomenology to conclude

that one could successfully accommodate a few TeV thermal dark matter candidate in agreement with direct detection and collider bounds. Our main results are summarized in Table IV.

ACKNOWLEDGMENTS

FSQ thanks Universidad Tecnica Frederico Santa Maria for the hospitality during the final states of this work. We thank Alfonso Zerwekh, Antonio Carcamo, and Carlos Pires for discussions. Y.S.V acknowledges the financial support of CAPES under Grant No. 88882.375870/2019-01. Y.M.O.T. acknowledges financial support from CAPES under grants 88887.485509 / 2020-00. FSQ is supported by ICTP-SAIR FAPESP grant 2016/01343-7, CNPq grants 303817/2018-6 and 421952/2018 – 0, and the Serrapilheira Foundation (grant number Serra - 1912 – 31613). LCD thanks Simons Foundation (Award Number: 884966, AF) for the financial support. S.K. is supported by ANID PIA/APOYO AFB180002 (Chile) and by ANID FONDECYT (Chile) No. 1190845. F.S.Q. and S.K. acknowledge support from ANID–Millennium Program–ICN2019_044 (Chile). AA is supported by CNPq (307317/2021-8). AA and FSQ also acknowledge support from FAPESP (2021/01089-1) grant.

-
- [1] G. Arcadi, M. Dutra, P. Ghosh, M. Lindner, Y. Mambrini, M. Pierre, S. Profumo, and F. S. Queiroz, *Eur. Phys. J. C* **78**, 203 (2018), arXiv:1703.07364 [hep-ph].
- [2] J. C. Montero, C. A. de S. Pires, and V. Pleitez, *Phys. Lett.* **B502**, 167 (2001), arXiv:hep-ph/0011296 [hep-ph].
- [3] M. B. Tully and G. C. Joshi, *Phys. Rev.* **D64**, 011301 (2001), arXiv:hep-ph/0011172 [hep-ph].
- [4] J. C. Montero, C. A. De S. Pires, and V. Pleitez, *Phys. Rev.* **D65**, 095001 (2002), arXiv:hep-ph/0112246 [hep-ph].
- [5] N. V. Cortez and M. D. Tonasse, *Phys. Rev.* **D72**, 073005 (2005), arXiv:hep-ph/0510143 [hep-ph].
- [6] D. Cogollo, H. Diniz, and C. A. de S. Pires, *Phys. Lett.* **B677**, 338 (2009), arXiv:0903.0370 [hep-ph].
- [7] D. Cogollo, H. Diniz, and C. A. de S. Pires, *Phys. Lett.* **B687**, 400 (2010), arXiv:1002.1944 [hep-ph].
- [8] D. Cogollo, H. Diniz, C. A. de S. Pires, and P. S. Rodrigues da Silva, *Eur. Phys. J.* **C58**, 455 (2008), arXiv:0806.3087 [hep-ph].
- [9] H. Okada, N. Okada, and Y. Orikasa, *Phys. Rev.* **D93**, 073006 (2016), arXiv:1504.01204 [hep-ph].
- [10] V. V. Vien, H. N. Long, and A. E. Cárcamo Hernández, *Mod. Phys. Lett.* **A34**, 1950005 (2019), arXiv:1812.07263 [hep-ph].
- [11] A. E. Cárcamo Hernández, H. N. Long, and V. V. Vien, *Eur. Phys. J.* **C78**, 804 (2018), arXiv:1803.01636 [hep-ph].
- [12] T. P. Nguyen, T. T. Le, T. T. Hong, and L. T. Hue, *Phys. Rev.* **D97**, 073003 (2018), arXiv:1802.00429 [hep-ph].
- [13] C. A. de Sousa Pires, F. Ferreira De Freitas, J. Shu, L. Huang, and P. Wagner Vasconcelos Olegário, *Phys. Lett.* **B797**, 134827 (2019), arXiv:1812.10570 [hep-ph].
- [14] A. E. Cárcamo Hernández, N. A. Pérez-Julve, and Y. Hidalgo Velásquez, *Phys. Rev.* **D100**, 095025 (2019), arXiv:1907.13083 [hep-ph].
- [15] A. E. Cárcamo Hernández, Y. Hidalgo Velásquez, and N. A. Pérez-Julve, *Eur. Phys. J.* **C79**, 828 (2019), arXiv:1905.02323 [hep-ph].
- [16] A. E. C. Hernández, L. T. Hue, S. Kovalenko, and H. N. Long, “An extended 3-3-1 model with two scalar triplets and linear seesaw mechanism,” (2021), arXiv:2001.01748 [hep-ph].
- [17] D. Fregolente and M. D. Tonasse, *Phys. Lett.* **B555**, 7 (2003), arXiv:hep-ph/0209119 [hep-ph].
- [18] H. N. Long and N. Q. Lan, *Europhys. Lett.* **64**, 571 (2003), arXiv:hep-ph/0309038 [hep-ph].
- [19] C. A. de S. Pires and P. S. Rodrigues da Silva, *JCAP* **0712**, 012 (2007), arXiv:0710.2104 [hep-ph].
- [20] J. K. Mizukoshi, C. A. de S. Pires, F. S. Queiroz, and P. S. Rodrigues da Silva, *Phys. Rev.* **D83**, 065024 (2011), arXiv:1010.4097 [hep-ph].
- [21] J. D. Ruiz-Alvarez, C. A. de S. Pires, F. S. Queiroz, D. Restrepo, and P. S. Rodrigues da Silva, *Phys. Rev. D* **86**, 075011 (2012), arXiv:1206.5779 [hep-ph].
- [22] S. Profumo and F. S. Queiroz, *Eur. Phys. J.* **C74**, 2960 (2014), arXiv:1307.7802 [hep-ph].
- [23] P. V. Dong, T. P. Nguyen, and D. V. Soa, *Phys. Rev.* **D88**, 095014 (2013), arXiv:1308.4097 [hep-ph].
- [24] P. V. Dong, H. T. Hung, and T. D. Tham, *Phys. Rev.* **D87**, 115003 (2013), arXiv:1305.0369 [hep-ph].
- [25] D. Cogollo, A. X. Gonzalez-Morales, F. S. Queiroz, and P. R. Teles, *JCAP* **1411**, 002 (2014), arXiv:1402.3271 [hep-ph].
- [26] P. V. Dong, D. T. Huong, F. S. Queiroz, and N. T. Thuy, *Phys. Rev.* **D90**, 075021 (2014), arXiv:1405.2591 [hep-ph].
- [27] P. V. Dong, N. T. K. Ngan, and D. V. Soa, *Phys. Rev.* **D90**, 075019 (2014), arXiv:1407.3839 [hep-ph].
- [28] C. Kelso, H. N. Long, R. Martinez, and F. S. Queiroz, *Phys. Rev. D* **90**, 113011 (2014), arXiv:1408.6203 [hep-ph].
- [29] Y. Mambrini, S. Profumo, and F. S. Queiroz, *Phys. Lett. B* **760**, 807 (2016), arXiv:1508.06635 [hep-ph].

- [30] P. V. Dong, C. S. Kim, D. V. Soa, and N. T. Thuy, *Phys. Rev. D* **91**, 115019 (2015), arXiv:1501.04385 [hep-ph].
- [31] C. A. de S. Pires, P. S. Rodrigues da Silva, A. C. O. Santos, and C. Siqueira, *Phys. Rev. D* **94**, 055014 (2016), arXiv:1606.01853 [hep-ph].
- [32] A. Alves, G. Arcadi, P. V. Dong, L. Duarte, F. S. Queiroz, and J. W. F. Valle, *Phys. Lett. B* **772**, 825 (2017), arXiv:1612.04383 [hep-ph].
- [33] P. S. Rodrigues da Silva, *Phys. Int.* **7**, 15 (2016), arXiv:1412.8633 [hep-ph].
- [34] C. D. R. Carvajal, B. L. Sánchez-Vega, and O. Zapata, *Phys. Rev. D* **96**, 115035 (2017), arXiv:1704.08340 [hep-ph].
- [35] P. V. Dong, D. T. Huong, F. S. Queiroz, J. W. F. Valle, and C. A. Vaquera-Araujo, *JHEP* **04**, 143 (2018), arXiv:1710.06951 [hep-ph].
- [36] G. Arcadi, C. P. Ferreira, F. Goertz, M. M. Guzzo, F. S. Queiroz, and A. C. O. Santos, *Phys. Rev. D* **97**, 075022 (2018), arXiv:1712.02373 [hep-ph].
- [37] J. C. Montero, A. Romero, and B. L. Sánchez-Vega, *Phys. Rev. D* **97**, 063015 (2018), arXiv:1709.04535 [hep-ph].
- [38] D. T. Huong, D. N. Dinh, L. D. Thien, and P. Van Dong, *JHEP* **08**, 051 (2019), arXiv:1906.05240 [hep-ph].
- [39] C. E. Alvarez-Salazar and O. L. G. Peres, *Phys. Rev. D* **103**, 035029 (2021), arXiv:1906.06444 [hep-ph].
- [40] D. Van Loi, C. H. Nam, and P. Van Dong, *Eur. Phys. J. C* **81**, 591 (2021), arXiv:2012.10979 [hep-ph].
- [41] M. Dutra, V. Oliveira, C. A. de S. Pires, and F. S. Queiroz, *JHEP* **10**, 005 (2021), arXiv:2104.14542 [hep-ph].
- [42] V. Oliveira and C. A. de S. Pires, (2021), arXiv:2112.03963 [hep-ph].
- [43] D. Cogollo, A. V. de Andrade, F. S. Queiroz, and P. Rebello Teles, *Eur. Phys. J. C* **72**, 2029 (2012), arXiv:1201.1268 [hep-ph].
- [44] D. Cogollo, F. S. Queiroz, and P. Vasconcelos, *Mod. Phys. Lett. A* **29**, 1450173 (2014), arXiv:1312.0304 [hep-ph].
- [45] A. J. Buras, F. De Fazio, and J. Girrbach-Noe, *JHEP* **08**, 039 (2014), arXiv:1405.3850 [hep-ph].
- [46] A. J. Buras and F. De Fazio, *JHEP* **03**, 010 (2016), arXiv:1512.02869 [hep-ph].
- [47] F. S. Queiroz, C. Siqueira, and J. W. F. Valle, *Phys. Lett. B* **763**, 269 (2016), arXiv:1608.07295 [hep-ph].
- [48] T. B. de Melo, S. Kovalenko, F. S. Queiroz, C. Siqueira, and Y. S. Villamizar, *Phys. Rev. D* **103**, 115001 (2021), arXiv:2102.06262 [hep-ph].
- [49] A. J. Buras and F. De Fazio, *JHEP* **08**, 115 (2016), arXiv:1604.02344 [hep-ph].
- [50] A. J. Buras, P. Colangelo, F. De Fazio, and F. Lopalco, *JHEP* **10**, 021 (2021), arXiv:2107.10866 [hep-ph].
- [51] J. M. Cabarcas, J. Duarte, and J. A. Rodriguez, 11th International Conference on Heavy Quarks and Leptons, *PoS HQL2012*, 072 (2012), arXiv:1212.3586 [hep-ph].
- [52] L. T. Hue, L. D. Ninh, T. T. Thuc, and N. T. T. Dat, *Eur. Phys. J. C* **78**, 128 (2018), arXiv:1708.09723 [hep-ph].
- [53] J. C. Montero and B. L. Sanchez-Vega, *Phys. Rev. D* **84**, 055019 (2011), arXiv:1102.5374 [hep-ph].
- [54] A. C. O. Santos and P. Vasconcelos, *Adv. High Energy Phys.* **2018**, 9132381 (2018), arXiv:1708.03955 [hep-ph].
- [55] E. R. Barreto, A. G. Dias, J. Leite, C. C. Nishi, R. L. N. Oliveira, and W. C. Vieira, *Phys. Rev. D* **97**, 055047 (2018), arXiv:1709.09946 [hep-ph].
- [56] G. De Conto, A. C. B. Machado, and J. P. B. C. de Melo, *Phys. Lett. B* **784**, 255 (2018), arXiv:1711.06718 [hep-ph].
- [57] N. Chen, Y. Liu, and Z. Teng, *Phys. Rev. D* **104**, 115011 (2021), arXiv:2106.00223 [hep-ph].
- [58] N. Chen, Y.-n. Mao, and Z. Teng, (2021), arXiv:2112.14509 [hep-ph].
- [59] M. Lindner, M. Platscher, and F. S. Queiroz, *Phys. Rept.* **731**, 1 (2018), arXiv:1610.06587 [hep-ph].
- [60] A. C. B. Machado, J. Montaña, and V. Pleitez, *J. Phys. G* **46**, 115005 (2019), arXiv:1604.08539 [hep-ph].
- [61] E. Ramirez Barreto, Y. do Amaral Coutinho, and J. Sa Borges, *Eur. Phys. J. C* **50**, 909 (2007), arXiv:hep-ph/0703099.
- [62] E. Ramirez Barreto, Y. A. Coutinho, and J. Sa Borges, *Phys. Lett. B* **689**, 36 (2010), arXiv:1004.3269 [hep-ph].
- [63] G. Corcella, C. Coriano, A. Costantini, and P. H. Frampton, *Phys. Lett. B* **773**, 544 (2017), arXiv:1707.01381 [hep-ph].
- [64] E. Ramirez Barreto, Y. A. Coutinho, and J. S. Borges, *Phys. Rev. D* **88**, 035016 (2013), arXiv:1307.4683 [hep-ph].
- [65] Y. A. Coutinho, V. Salustino Guimarães, and A. A. Nepomuceno, *Phys. Rev. D* **87**, 115014 (2013), arXiv:1304.7907 [hep-ph].
- [66] A. Nepomuceno and B. Meirose, *Phys. Rev. D* **101**, 035017 (2020), arXiv:1911.12783 [hep-ph].
- [67] A. S. De Jesus, S. Kovalenko, F. S. Queiroz, C. Siqueira, and K. Sinha, *Phys. Rev. D* **102**, 035004 (2020), arXiv:2004.01200 [hep-ph].
- [68] A. Collaboration et al., *Physics Letters B* **796**, 68 (2019).
- [69] H. N. Long, *Physical Review D* **54**, 4691 (1996), arXiv:hep-ph/9607439 [hep-ph].
- [70] H. N. Long, *Phys. Rev. D* **53**, 437 (1996), arXiv:hep-ph/9504274 [hep-ph].
- [71] M. E. Catano, R. Martinez, and F. Ochoa, *Phys. Rev. D* **86**, 073015 (2012), arXiv:1206.1966 [hep-ph].
- [72] A. Pukhov, A. Belyaev, and N. Christensen, “Calchep,” <https://theory.sinp.msu.ru/~pukhov/calchep.html> (Accessed: 2021-09-20).
- [73] J. Alwall, R. Frederix, S. Frixione, V. Hirschi, F. Maltoni, O. Mattelaer, H.-S. Shao, T. Stelzer, P. Torrielli, and M. Zaro, *Journal of High Energy Physics* **2014**, 1 (2014), arXiv:1405.0301 [hep-ph].
- [74] R. Frederix, S. Frixione, V. Hirschi, D. Pagani, H.-S. Shao, and M. Zaro, *Journal of High Energy Physics* **2018**, 1 (2018), arXiv:1804.10017 [hep-ph].
- [75] A. Belyaev, N. D. Christensen, and A. Pukhov, *Computer Physics Communications* **184**, 1729 (2013), arXiv:1207.6082 [hep-ph].
- [76] S. Carrazza, S. Forte, and J. Rojo, in *43rd International Symposium on Multiparticle Dynamics* (2013) pp. 89–96, arXiv:1311.5887 [hep-ph].
- [77] A. Semenov, *Computer physics communications* **115**, 124 (1998).
- [78] A. Semenov, *Computer Physics Communications* **180**, 431 (2009).
- [79] A. Semenov, *Computer Physics Communications* **201**, 167 (2016).
- [80] F. Staub, “Sarah,” <https://sarah.hepforge.org/> (Accessed: 2020-03-20).
- [81] A. Vicente, “Computer tools in particle physics,” (2017), arXiv:1507.06349 [hep-ph].
- [82] F. Staub, *Advances in High Energy Physics* **2015** (2015), 10.1155/2015/840780.
- [83] A. Alloul, N. D. Christensen, C. Degrande, C. Duhr, and B. Fuks, *Computer Physics Communications* **185**, 2250 (2014), arXiv:1310.1921 [hep-ph].
- [84] A. Alloul, N. D. Christensen, C. Degrande, C. Duhr, and B. Fuks, “Feynrules,” <https://feynrules.irmp.ucl.ac.be/> (Accessed: 2021-09-20).

- [85] M. Cepeda *et al.*, *CERN Yellow Rep. Monogr.* **7**, 221 (2019), [arXiv:1902.00134 \[hep-ph\]](#).
- [86] A. Abada *et al.* (FCC), *Eur. Phys. J. C* **79**, 474 (2019).
- [87] A. G. Dias, C. A. de S. Pires, and P. S. Rodrigues da Silva, *Phys. Lett. B* **628**, 85 (2005), [arXiv:hep-ph/0508186](#).
- [88] L. A. Harland-Lang, A. D. Martin, P. Motylinski, and R. S. Thorne, *Eur. Phys. J. C* **75**, 204 (2015), [arXiv:1412.3989 \[hep-ph\]](#).
- [89] N. Aghanim *et al.* (Planck), *Astron. Astrophys.* **641**, A6 (2020), [Erratum: *Astron. Astrophys.* 652, C4 (2021)], [arXiv:1807.06209 \[astro-ph.CO\]](#).
- [90] A. Alves, S. Profumo, and F. S. Queiroz, *JHEP* **04**, 063 (2014), [arXiv:1312.5281 \[hep-ph\]](#).
- [91] A. Alves, A. Berlin, S. Profumo, and F. S. Queiroz, *Phys. Rev. D* **92**, 083004 (2015), [arXiv:1501.03490 \[hep-ph\]](#).
- [92] E. Aprile *et al.* (XENON), *Phys. Rev. Lett.* **121**, 111302 (2018), [arXiv:1805.12562 \[astro-ph.CO\]](#).
- [93] Y. Meng *et al.* (PandaX-4T), *Phys. Rev. Lett.* **127**, 261802 (2021), [arXiv:2107.13438 \[hep-ex\]](#).
- [94] E. Aprile *et al.* (XENON), *JCAP* **11**, 031 (2020), [arXiv:2007.08796 \[physics.ins-det\]](#).
- [95] G. Salam and A. Weiler, “Collider reach (β),” <http://collider-reach.web.cern.ch/> (Accessed: 2021-09-21).
- [96] Q.-H. Cao and D.-M. Zhang, “Collider phenomenology of the 3-3-1 model,” (2016), [arXiv:1611.09337 \[hep-ph\]](#).
- [97] S. Profumo and F. S. Queiroz, *The European Physical Journal C* **74**, 1 (2014).
- [98] P. D. Group *et al.*, *Progress of Theoretical and Experimental Physics* **2020**, 1 (2020).